Int J Clin Exp Med 2020;13(4):2250-2258
www.ijcem.com /ISSN:1940-5901/IJCEM0103050

Original Article

Novel multi-target nanoparticles contrast agent cooperated with MRI in early-stage prostate cancer

Peijing Lv[1*], Fajun Ju[2*], Linghong Meng[3], Jiangwei Xie[2], Deke Sun[4], Tao Yang[2], Yueqin Chen[5]

[1]Department of Imaging, Ji'ning Hospital of Traditional Chinese Medicine, Ji'ning, Shandong Province, China; Departments of [2]Imaging, [4]Neurosurgery, Yishui Central Hospital, Linyi, Shandong Province, China; [3]Department of Radiology, The People's Hospital of Zoucheng City, Zoucheng, Shandong Province, China; [5]Department of Imaging, Affiliated Hospital of Ji'ning Medical University, Ji'ning, Shandong Province, China. [*]Co-first authors and equal contributors.

Received October 1, 2019; Accepted November 7, 2019; Epub April 15, 2020; Published April 30, 2020

Abstract: Objective: To evaluate the application value of novel multi-target nanoparticles lenvatinib contrast agent (lenvatinib) combined with magnetic resonance imaging (MTNCA-MRI) in diagnosis of patients with early-stage prostate cancer. Methods: Lenvatinib were packaged into multi-target nanoparticles as MTNCA to clot prostate cancer cells during MRI detection (MTNCA-MRI). A total of 286 patients with suspected early-stage prostate cancer (PSA ≥20 μg/mL) were recruited and equally divided into MTNCA-MRI group and MRI group. Prostate cancer cell line and normal cell as well as plasma samples from 42 prostate cancer patients and 10 healthy volunteers were applied to observe the potential of MTNCA (lenvatinib) in target diagnosis and treatment in patients with prostate cancer. The efficacy of MTNCA-MRI was investigated and the pharmacodynamics of MTNCA and prognosis of patients with prostate cancer diagnosed by MTNCA-MRI were also analyzed. Results: Western blot indicated that the expressions of VEGFR, FGFR, Ret, KIT and PDGFR-β were upregulated in prostate cancer cells compared with normal prostate cells (all $P<0.05$). Immunofluorescence indicated that FITC-labeled MTNCA is able to bind with PC-3 cells and the minimum dose of MTNCA to achieve the optimum signal intensity for MRI detection was 24 mg/kg. MTNCA-MRI successfully diagnosed 86 patients with prostate cancer, whereas prostate cancer was confirmed in only 49 patients using MRI ($P<0.01$). The plasma level of MTNCA was increased at 4 h post-treatment and MTNCA was metabolized within 24 h (<10 ng/mL). The survival rate of patients with early-stage prostate cancer detected by MTNCA-MRI was higher compared to the patients detected by MTNCA-MRI only ($P<0.01$). Conclusion: MTNCA-MRI may be a potential future diagnostic method for clinical assessment of patients with suspected early-stage prostate cancer.

Keywords: Prostate cancer, magnetic resonance imaging, early diagnosis, lenvatinib, tyrosine kinase inhibitor

Introduction

Well-recognized as the most frequently diagnosed malignancy in males, prostate cancer has high morbidity and mortality rates (4.7 and 1.0 in 100,000, respectively) [1]. Early diagnosis and treatment for prostate cancer is essential for improvements in therapeutic effect and survival time [2]. At present, serum total prostate specific antigen (PSA) is widely used to screen patients with prostate cancer as a PSA of 4-10 ng/mL is regarded as the threshold value for a positive prostate cancer diagnosis [3]. However, it has been demonstrated the false positive rate for PSA based diagnosis is over 17% in clinic and 23-42% of screen-detected prostate cancers are over-treated [4-6]. Prostate biopsy to detecting prostate cancer increases anxiety and distress in men undergoing active surveillance, thereby is often refused [7].

In recent years, magnetic resonance imaging (MRI) has been widely used for the diagnosis of prostate cancer as it is advantageous over other diagnostic methods in resolution of the image and image quality [8-10]. MRI usually combines with other methods in the clinical diagnosis of cancer. For example, Lee et al. investigated the diagnostic value of integrated positron emission topography (PET) and MRI for the detection and localization of prostate cancer in the clinic, of which the results showed that the combination method could increase

Table 1. Characteristics of subjects with suspected prostate cancer

Characteristics	MTNCA-MRI	MRI	t/χ^2	P
Number of patients	143	143		
Age (years)	51.1±1.2	50.9±1.5	1.245	0.214
Patients with a history of cancer (n, %)	2 (1.4%)	2 (1.4%)		
Blood pressure (mmHg)	114.24±12.02	113.94±13.88	0.195	0.845
Blood glucose (mmol/L)	7.18±1.42	6.89±1.32	1.789	0.075

Note: All patients underwent magnetic resonance imaging (MRI) and multi-target nanoparticle contrast agent-MRI (MTNCA-MRI). MRI: magnetic resonance imaging; MTNCA: multi-target nanoparticle contrast agent.

the rate of accurate diagnosis [11]. However, these approaches with current diagnostic accuracy and sensitivity are insufficient to diagnose patients with early stage prostate cancer.

Lenvatinib, a kind of multiple targets tyrosine enzyme inhibitor, could inhibit the growth of tumor via several signal pathways, such as vascular endothelial growth factor receptors (VEGFRs), fibroblast growth factor receptors (FGFR), platelet-derived growth factor receptor (PDGFR-α/β), receptor tyrosine Kinase receptor (RET) and mast/stem cell growth factor receptor (KIT); therefore, lenvatinib gradually began to be used in the treatment of various advanced tumors and the results showed that it has certain clinical effect [12, 13].

In the present study, a novel multi-target nanoparticles contrast agent (lenvatinib) combined with MRI (MTNCA-MRI) was applied in order to improve the accuracy and sensitivity of MRI in the diagnosis of prostate cancer, with the hope to provide more data for the diagnosis of early-stage prostate cancer in clinic.

Material and methods

Patients

A total of 286 male subjects with suspected prostate cancer (PSA ≥20 μg/mL) aged 36.4-74.8 years were recruited for the current study between August 2011 and May 2014 from Affiliated Hospital of Ji'ning Medical University. They were equally divided into MTNCA-MRI group and MRI group according to the random number table. There were no differences in the basic information between the two groups (**Table 1**). Meanwhile, a total of 10 (male; mean age: 42.4 years old) healthy volunteers and 42 patients with prostate cancer (male; mean age: 40.8 years old) who were diagnosed by pathology were also enrolled in the present study. The present study was approved by the Ethics Committee of Affiliated Hospital of Ji'ning Medical University. Clinical trials were performed in strict accordance with the recommendations in the Guide for the Care and Use of Clinical Study of China. (BUCMT20070612M25) [14].

Experiment design

Prostate cancer cell line and normal cells as well as plasma samples from 42 prostate cancer patients and 10 healthy volunteers were applied to investigate the difference of tyrosine kinase receptors between these two groups, so as to observe whether the MTNCA (lenvatinib) has the potential for the target diagnosis and treatment in patients with prostate cancer. Subsequently, we prepared MTNCA and subjects in MTNCA-MRI group were underwent MRI after the MTNCA administration, while the subjects in MRI group were underwent MRI only; for the subjects diagnosed by the two methods, puncture and biopsy were performed to confirm the diagnostic results. Then the diagnostic effects of MTNCA-MRI and MRI imaging methods were compared. Additionally, in order to assess the accuracy of MTNCA-MRI, signal intensity was detected following the administration of MTNCA in subjects with suspected prostate cancer. Moreover, the pharmacodynamics of MTNCA and its targets were investigated to observe and verify the metabolism and safety of MTNCA. Finally, prognosis of patients with prostate cancer diagnosed by MTNCA-MRI was observed.

Preparation of MTNCA and administration

Lenvatinib contrast agent (Sunbio, Inc., Gunpo, Korea) was bound with the nanoparticles of superparamagnetic iron oxide particles using covalent bonds, as previously described, which adhered to tumor lesions in the urinary system [15]. A total of 42 patients were randomly cho-

Table 2. Determination of minimum dosage of MTNCA for patients with prostate cancer

Parameters	MTNCA Dosage (mg/kg)		
	10-16 (n=10)	18-24 (n=14)	26-32 (n=18)
Signal intensity (%)	23.2±7.8	73.2±14.4	74.5±14.8
Sensitive (%)	34.8±6.6	81.6±12.6	80.5±13.2

Note: MTNCA: multi-target nanoparticle contrast agent.

Table 3. Treatment strategies used for patients with prostate cancer diagnosed by MTNCA-MRI

Treatment strategies	MTNCA-MRI	MRI	χ^2	P
Total number	86	49		
Treatments			0.026	1.000
Radiotherapy	31	18		
Chemotherapy	11	6		
Chinese medicine	18	10		
Biological therapy	10	6		
Comprehensive therapy	16	9		

Note: MRI: magnetic resonance imaging; MTNCA: multi-target nanoparticle contrast agent.

sen to determine the minimum dose of MTNCA according to the minimum signal intensity and sensitivity [16]. The prepared nanoparticles contrast agent (lenvatinib; 10, 16, 18, 24, 26 and 32 mg/kg) was visualized using an MRI system and administered via intravenous injection 30 min prior to MRI (**Table 2**). The optimum signal intensity was determined by image quality and resolution.

MRI scanning

The MRI diagnosis system (Ingenia 3.0 T; Philips Medical Systems, Cleveland, OH, USA) was used to diagnose patients with suspected prostate cancer using a preprogrammed setting which was optimized to reach the best image formation. MRI was performed on the prostate and its affiliated structure in all patients according to the manufacturer's protocol. Details of the principles and settings of MRI are described in a previous study [17].

Image analysis

Outcomes generated by MTNCA-MRI and MRI image sets were analyzed using the software provided with the MRI system. Subjects with suspected early-stage prostate cancer were analyzed using a preprogrammed program and the prostate cancer masses were diagnosed using MTNCA-MRI or MRI images. The number of tiny prostate cancer tumor nodules was automatically calculated by drawing regions of tumor lesions using Sante MRI Viewer software (version 3.2; Siemens Healthineers, Erlangen, Germany). Signal enhancement of MRI induced by MTNCA was also measured using a preprogrammed program on the MRI system. The peripheral zone of normal prostate has crescent shape and uniform and high signal in T2WI, which will appear isolated or multiple low-signal nodules when cancer occurs [18].

Treatment of patients diagnosed with prostate cancer by MTNCA-MRI and MRI only

Patients with suspected early-stage prostate cancer diagnosed by MTNCA-MRI and MRI were confirmed by pathology. They received different treatments according to their personal conditions, including radiotherapy, chemotherapy, Traditional Chinese Medicine, biological therapy and comprehensive therapy following surgery (**Table 3**). Median overall survival and median progression-free survival were analyzed according to a previously published protocol [19].

Cells and reagents

Prostate cancer cell line PC-3 and normal prostate cell line 22RV1 were purchased from the American Type Culture Collection (Manassas, VA, USA). PC-3 cells were cultured in Dulbecco's modified Eagle's medium (Sigma-Aldrich, USA) supplemented with 10% fetal bovine serum (Thermo Fisher Scientific, USA). 22RV1 cells were cultured in RPMI 1640 medium (Thermo Fisher Scientific, USA) supplemented with 10% FBS. All cells were cultured for 24 h in an incubator with 5% CO_2 at 37°C.

Enzyme-linked immunosorbent assay

Plasma concentration levels of VEGFR (Abcam, Cambridge, UK), FGFR (Abcam, Cambridge, UK), Ret (Shanghai Jinkang Biological Engineering Co., Ltd., Shanghai, China), KIT (Sino Biological Inc., Beijing, China), Lenvatinib (Selleck Chemicals LLC, USA) and PDGFR-β (R&D Systems China Co., Ltd., Shanghai, China) in patients with prostate cancer and healthy volunteers were analyzed using commercialized ELISA kits according to the manufacturer's protocol. The results were analyzed by using an

ELISA reader system (Bio-Rad Laboratories, Inc., Hercules, CA, USA).

Western blot analysis

Cells were homogenized and centrifuged at 8,000 g at 4°C for 10 min. Protein concentration was measured by a BCA protein assay kit (Thermo Fisher Scientific, Inc.). Protein samples (20 μg/lane) were separated by 15% SDS-PAGE and then transferred to a polyvinylidene fluoride membrane (EMD Millipore, Billerica, MA, USA). For western blotting, rabbit anti-human VEGFR (Abcam, Cambridge, UK), rabbit anti-human FGFR (Abcam, Cambridge, UK), rabbit anti-human Ret (Abcam, Cambridge, UK), rabbit anti-human KIT (Abcam, Cambridge, UK), mouse anti-human PDGFR-β (Santa Cruz Biotechnology, CA, USA) and mouse anti-human β-actin (Santa Cruz Biotechnology, CA, USA) antibodies were added and incubated overnight at 4°C following blocking with 5% skimmed milk for 1 h at 37°C. The membranes were then incubated with corresponding horseradish peroxidase (HRP)-conjugated-immunoglobulin (Ig) G secondary antibodies (Santa Cruz Biotechnology, CA, USA) for 4 h at 4°C. The membranes were washed three times with 0.1% Tween 20 in Tris buffer solution (Sigma-Aldrich; Merck KGaA), then bound proteins were developed using RapidStep™ ECL Reagent (EMD Millipore, Billerica, MA, USA) and detected with a bio-imaging system. Densitometric quantification of the western blotting data was performed using Quantity-One software (version 3.23; Bio-Rad Laboratories, Inc.).

Immunofluorescence staining

Prostate cancer PC-3 cells were incubated with fluorescein isothiocyanate (FITC)-labeled MTNCA for 2 h at 37°C. The FITC-labeled lenvatinib was applied as control. Cells were washed three times with PBS and observed using a fluorescence microscope (400 X). Procedures were performed according to a previously published protocol [20].

Statistical analysis

The data of this study were analyzed by SPSS 19.0 statistical software. All data are presented as the mean ± standard deviation and experiments were performed in triplicate. Unpaired data was analyzed using a student's t test and multiple group comparisons were performed using one-way analysis of variance followed by Dunnett's test. Kaplan-Meier test was used to estimate the survival rate during the 60-month long-term observation. $P<0.05$ was considered to indicate statistically significant differences.

Results

The expression of tyrosine kinase in prostate cancer cells and plasma from patients

As shown in **Figure 1**, VEGFR and FGFR plasma levels were significantly upregulated in patients with prostate cancer compared with healthy volunteers (both $P<0.05$, **Figure 1A**, **1B**); however, no significant differences were observed in the plasma levels of Ret, KIT or PDGFR-β between patients with prostate cancer and healthy volunteers (all $P>0.05$, **Figure 1C-E**). Western blot indicated that the expressions of VEGFR, FGFR, Ret, KIT and PDGFR-β were upregulated in prostate cancer cells compared with those in normal prostate cells (all $P<0.05$, **Figure 1F**).

Efficacy of MTNCA-MRI in early clinical diagnosis for patients with suspected prostate cancer

Immunofluorescence indicated that FITC-labeled MTNCA is able to bind with PC-3 cells (**Figure 2A**). The minimum dose of MTNCA to achieve the optimum signal intensity for MRI detection was identified as 24 mg/kg (**Table 2**).

Clinical analysis indicated that MTNCA-MRI diagnosed 86 (60.14%) patients with prostate cancer, while prostate cancer was confirmed in only 49 (34.26%) patients using MRI ($P<0.01$; **Figure 2B**). MTNCA decreased plasma levels of VEGFR and FGFR in patients with prostate cancer 4 h following MTNCA administration (both $P<0.01$, **Figure 2C**, **2D**). These outcomes suggest that MTNCA-MRI may be a promising early diagnostic method for subjects with suspected prostate cancer.

MTNCA improves signal intensity for MRI fed back from lesions in patients with prostate cancer

As shown in **Figure 3A**, MTNCA significantly enhanced signal intensity compared with MRI in the prostates of subjects with suspected prostate cancer up to 24 h following MTNCA administration (both $P<0.01$). The results also indicated that MTNCA was rapidly metabolized in the prostate, as the signal enhancement

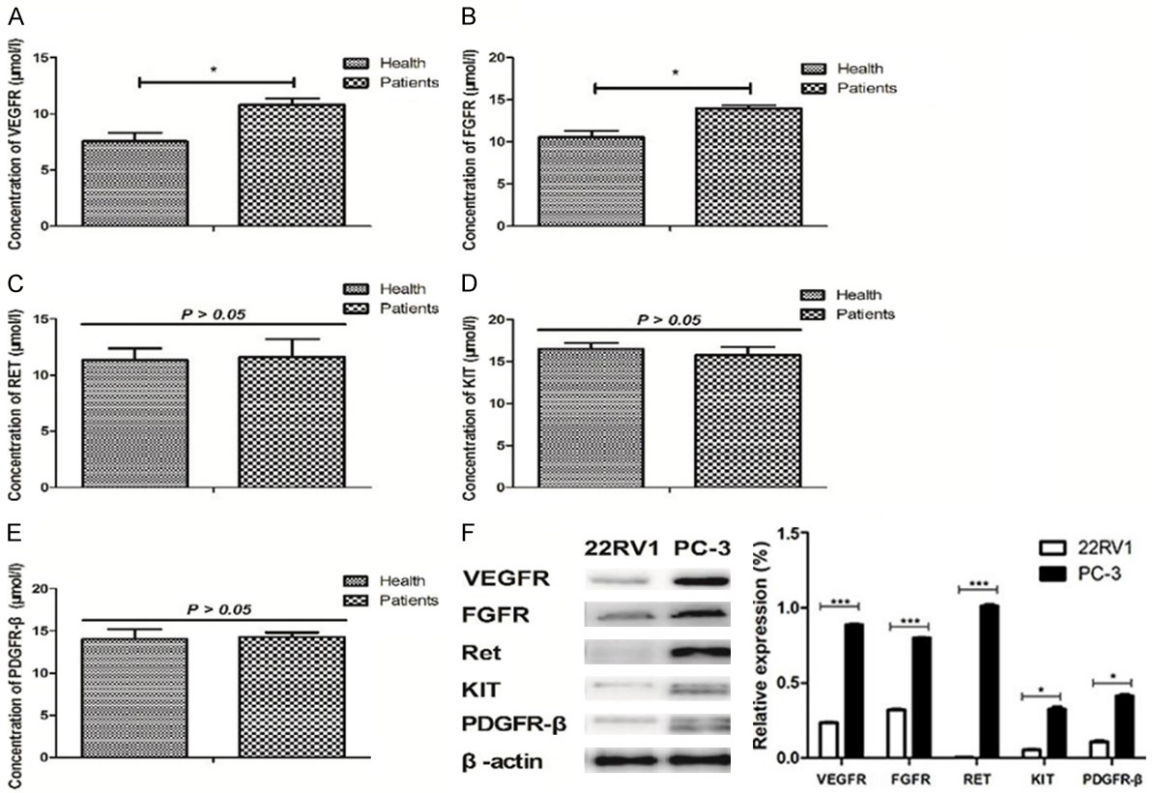

Figure 1. Analysis of the expression of tyrosine kinase inhibitors in plasma and prostate cancer cells. Plasma levels of (A) VEGFR, (B) FGFR, (C) Ret, (D) KIT and (E) PDGFR-β in patients with prostate cancer determined by ELISA. (F) Expression of VEGFR, FGFR, Ret, KIT and PDGFR-β in prostate cancer PC-3 cells and normal prostate 22RV1 cells. The experiments were performed in triplicate. *P<0.05, ***P<0.001. VEGFR: vascular endothelial growth factor receptor, FGFR: fibroblast growth factor receptor, Ret: receptor tyrosine kinase, KIT: mast/stem cell growth factor receptor, PDGFR-β: platelet-derived growth factor receptor-β.

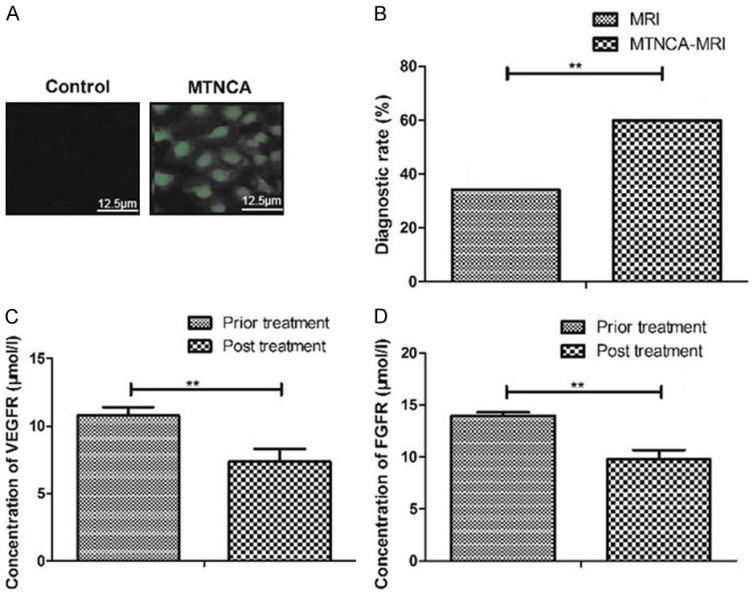

Figure 2. Efficacy of MTNCA-MRI in early clinical diagnosis of subjects with suspected prostate cancer. (A) Affinity of MTNCA for prostate cancer cell line PC-3 determined by immunofluorescence (400 X). (B) Diagnostic rate of MTNCA-MRI and MRI for patients with suspected prostate cancer. (C, D) Changes of plasma levels of VEGFR (C) and FGFR (D) in patients with prostate cancer following injection of MTNCA. **P<0.01. All experiments were performed in triplicate. VEGFR: vascular endothelial growth factor receptor, FGFR: fibroblast growth factor receptor, MRI: magnetic resonance imaging, MTNCA: multi-target nanoparticle contrast agent.

decreased in the prostate 72 h following MTNCA treatment (**Figure 3B**). Meanwhile, a stronger signal in the tumor nodules was observed in subjects following injection of MTNCA compared with MRI (**Figure 3C**). These outcomes suggest that MTNCA improves the signal intensity for MRI from lesions in patients with prostate cancer.

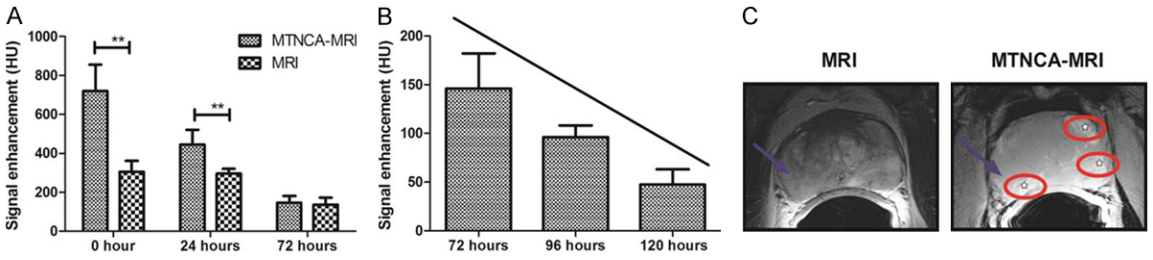

Figure 3. Effects of MTNCA on signal intensity for MRI fed back from lesions in patients with prostate cancer. A. Signal enhancement was significantly enhanced by MTNCA in lesions in patients with prostate cancer. **P<0.01. B. Attenuated signal of MTNCA was analyzed in patients with prostate cancer. C. Detection of prostate tumors following injection of MTNCA in the nodules. Blue arrows indicate the tumor lesions. Yellow stars inside red circles indicate the tumor regions. All experiments were performed in triplicate. MRI: magnetic resonance imaging, MTNCA: multi-target nanoparticle contrast agent.

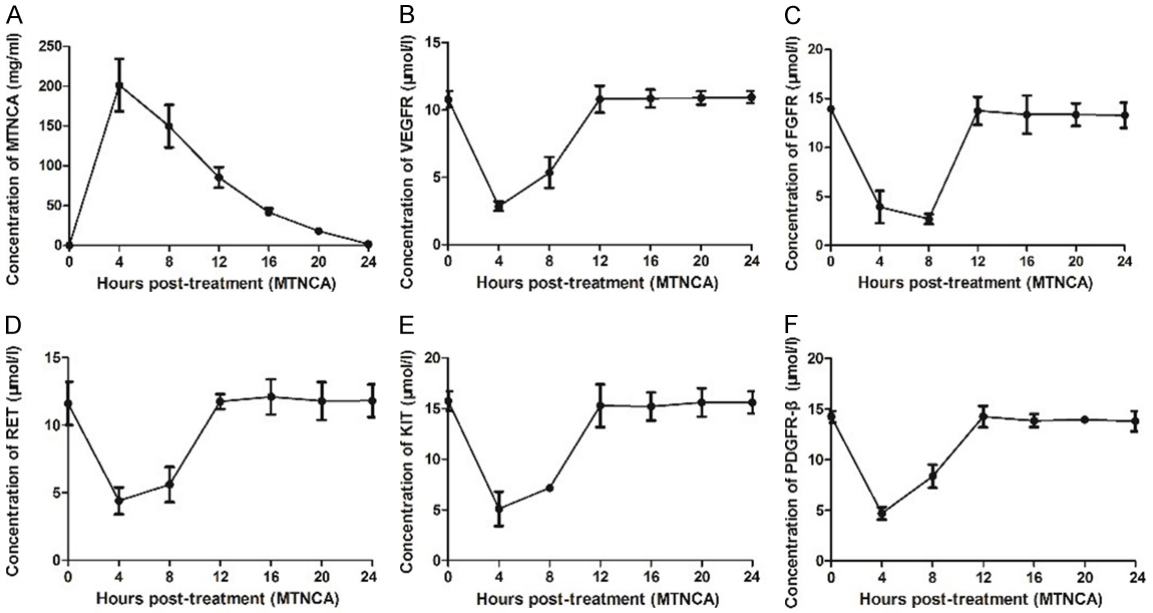

Figure 4. Pharmacodynamics of MTNCA and its targets in plasma in patients with early-stage prostate cancer. (A) Pharmacodynamics of MTNCA in plasma from patients with early-stage prostate cancer diagnosed by MTNCA-MRI. (B-E) Plasma concentration levels of (B) VEGFR, (C) FGFR, (D) Ret, (E) KIT and (F) PDGFR-β in patients with early-stage prostate cancer diagnosed using MTNCA-MRI. All experiments were performed in triplicate. VEGFR: vascular endothelial growth factor receptor, FGFR: fibroblast growth factor receptor, Ret receptor tyrosine Kinase, KIT: mast/stem cell growth factor receptor, PDGFR-β: platelet-derived growth factor receptor-β, MRI: magnetic resonance imaging, MTNCA: multi-target nanoparticle contrast agent.

Pharmacodynamics of MTNCA in plasma in patients with early-stage prostate cancer

The plasma level of MTNCA were increased at 4 h post-treatment and MTNCA was metabolized within 24 h (<10 ng/mL; **Figure 4A**). The plasma VEGFR, FGFR, Ret, KIT, and PDGFR-D were decreased 4 h post-treatment and recovered to normal levels within 12 h in patients with early stage prostate cancer diagnosed by MTNCA-MRI (**Figure 4B-F**).

Prognosis of patients with prostate cancer diagnosed by MTNCA-MRI

Patients with early-phase prostate cancer in the present study underwent different anti-cancer treatments and the two groups showed no evident difference (**Table 3**). Patients with early-stage prostate cancer diagnosed with MTNCA-MRI had a longer survival time and median progression-free survival compared with those diagnosed by MRI alone (both

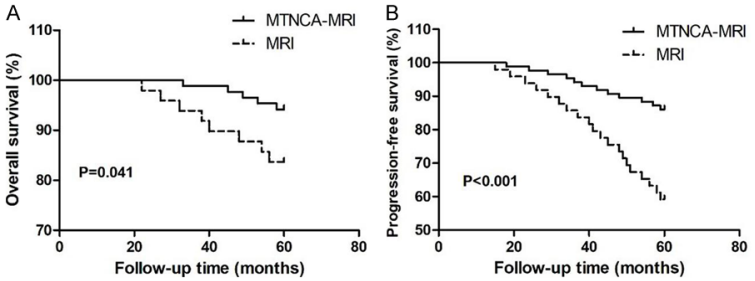

Figure 5. Survival rates of patients with early-stage prostate cancer diagnosed by MTNCA-MRI. A. Evaluation of the median overall survival of patients with early-stage prostate cancer diagnosed by MTNCA-MRI or MRI only. B. Analysis of the median progression-free survival of patients with early-stage prostate cancer diagnosed using MTNCA-MRI or MRI only. MRI: magnetic resonance imaging, MTNCA: multi-target nanoparticle contrast agent.

Table 4. Survival in patients with early-stage prostate cancer diagnosed by MTNCA-MRI or MRI only

Group	Cases	Tumor free	Survival with tumor	Succumbed
MTNCA-MRI	86	72	9	5
MRI	49	29	12	8
χ^2			10.040	
P			0.007	

Note: MRI: magnetic resonance imaging; MTNCA: multi-target nanoparticle contrast agent.

P<0.05, **Figure 5**). After the 60-month follow-up, the treatment effect was better in MTNCA-MRI group than MRI group (P=0.007, **Table 4**). Taken together, these outcomes suggest that using MTNCA-MRI to diagnose patients with early-phase prostate cancer may prolong their survival and progression-free survival period following the administration of anti-cancer treatments.

Discussion

Currently, lenvatinib has been used in thyroid cancer, kidney cancer, liver cancer and many other cancers. As a drug with multiple targets, lenvatinib blocks the activity of cancer cells in two ways: first, it could inhibit the tumor formation; second, it could suppress the angiogenesis and excessive growth signals to achieve tumor reduction [12, 21]. In our study, we found that compared with healthy subjects, lenvatinib could inhibit the expression of VEGFR, FGFR, Ret, KIT and PDGFR-β in prostate cancer cells and patients' plasma, indicating that VEGFR, FGFR, Ret, KIT and PDGFR-β may be regarded as potential biomarkers for the diagnosis of patients with pro state cancer, especially for VEGFR and FGFR.

Development of a non-invasive assay for the accurate diagnosis of progressive prostate cancer is of great significance and remains a clinical challenge [22, 23]. The feasibility ofspectralMRIimagingforthedetection of tumor lesions with target-based contrast agents has previously been demonstrated [24-29]. Several novel molecular imaging technologies have been developed for diagnosing prostate cancer [30-32]. In this study, lenvatinib was made into MTNCA and administrated to subjects before MRI was performed, and the diagnostic rate was significantly increased compared with MRI only. Moreover, the prognosis of MTNCA-MRI group was obviously better than that of MRI group. On the one hand, this could be because the bioavailability and targeted effect of lenvatinib was increased by nanoparticles, therefore, the diagnosis rate and prognosis are improved. The immunofluorescence staining results in this study found that MTNCA and prostate cancer cells had better affinity. Li et al. found that nanoparticle contrast agents can significantly improve the targeting of liver and spleen organs, which was consist with our results [33].

On the other hand, MTNCA can enhance MRI signal intensity. In our study, MTNCA significantly enhanced signal intensity compared with MRI in the prostates of subjects with suspected prostate cancer up to 24 h following MTNCA administration; meanwhile, a stronger signal in the tumor nodules was observed in subjects following injection of MTNCA compared with MRI. The prepared MTNCA in this study contained superparamagnetic iron oxide (SPIO) particles, which is a tumor probe with high efficiency [34, 35]. Numerous reports have proved that SPIO can improve the tumor detection rate in MRI [36-38]. These outcomes suggest that MTNCA improves the signal intensity

for MRI, thus improving the diagnosis effect of MRI.

Our study also found that the metabolism of MTNCA in vivo was fast, and the expression of related tyrosine kinases could be activated and recovered to normal levels within 12 h, suggesting that MTNCA may be a promising novel targeting nanoparticle contrast agent as it is metabolized in patients with early-stage prostate cancer diagnosed by MTNCA-MRI.

In conclusion, the application of novel MTNCA in combination with MRI improves diagnostic accuracy in patients with early-stage prostate cancer and the outcomes suggest that MTNCA-MRI may possess significant clinical value for diagnosing patients with suspected prostate cancer in the future. However, as the present study was a single center study with limited cases, more evidences are needed to support our findings in the future.

Disclosure of conflict of interest

None.

Address correspondence to: Linghong Meng, Department of Radiology, The People's Hospital of Zoucheng City, No.59 Qianquan Road, Zoucheng 273500, Shandong Province, China. Tel: +86-15065378543; E-mail: chenyueqin0306@163.com

References

[1] Feldman AS, Meyer CP, Sanchez A, Krasnova A, Reznor G, Menon M, Kibel AS, Choueiri TK, Lipsitz SR, Sun M and Trinh QD. Morbidity and mortality of locally advanced prostate cancer: a population based analysis comparing radical prostatectomy versus external beam radiation. J Urol 2017; 198: 1061-1068.

[2] Pan LH, Kuo SH, Lin TY, Lin CW, Fang PY and Yang HW. An electrochemical biosensor to simultaneously detect VEGF and PSA for early prostate cancer diagnosis based on graphene oxide/ssDNA/PLLA nanoparticles. Biosens Bioelectron 2017; 89: 598-605.

[3] Jemal A, Siegel R, Xu J and Ward E. Cancer statistics, 2010. CA Cancer J Clin 2010; 60: 277-300.

[4] Chen R, Sjoberg DD, Huang Y, Xie L, Zhou L, He D, Vickers AJ and Sun Y. Prostate specific antigen and prostate cancer in Chinese men undergoing initial prostate biopsies compared with western cohorts. J Urol 2017; 197: 90-96.

[5] Shoaibi A, Rao GA, Cai B, Rawl J, Haddock KS and Hebert JR. Prostate specific antigen-growth curve model to predict high-risk prostate cancer. Prostate 2017; 77: 173-184.

[6] Draisma G, Etzioni R, Tsodikov A, Mariotto A, Wever E, Gulati R, Feuer E and de Koning H. Lead time and overdiagnosis in prostate-specific antigen screening: importance of methods and context. J Natl Cancer Inst 2009; 101: 374-83.

[7] Dale W, Hemmerich J and Meltzer D. Extending the validity of the memorial anxiety scale for prostate cancer (MAX-PC) at the time of prostate biopsy in a racially-mixed population. Psychooncology 2007; 16: 493-8.

[8] Mennella S, Paparo F, Revelli M, Baccini P, Secondini L, Barbagallo S, Friedman D and Garlaschi A. Magnetic resonance imaging of breast cancer: does the time interval between biopsy and MRI influence MRI-pathology discordance in lesion sizing? Acta Radiol 2017; 58: 800-808.

[9] Vargas HA, Schor-Bardach R, Long N, Kirzner AN, Cunningham JD, Goldman DA, Moskowitz CS, Sosa RE, Sala E, Panicek DM and Hricak H. Prostate cancer bone metastases on staging prostate MRI: prevalence and clinical features associated with their diagnosis. Abdom Radiol (NY) 2017; 42: 271-277.

[10] Moore CM and Taneja SS. Integrating MRI for the diagnosis of prostate cancer. Curr Opin Urol 2016; 26: 466-71.

[11] Lee MS, Cho JY, Kim SY, Cheon GJ, Moon MH, Oh S, Lee J, Lee S, Woo S and Kim SH. Diagnostic value of integrated PET/MRI for detection and localization of prostate cancer: comparative study of multiparametric MRI and PET/CT. J Magn Reson Imaging 2017; 45: 597-609.

[12] Zhang BY, Gu JZ and Guo Y. Clinical research progress of lovastinib in the treatment of advanced tumors. Chinese Journal of New Drugs 2018.

[13] Wang LX, Xiao D and Zhou XB. An oral multiple receptor tyrosine kinase inhibitor-Lenvatinib. Clinical Medication Journal 2015; 13: 11-14.

[14] Wang Q, Li J, Zheng S, Li JY, Pang Y, Huang R, Zhang BN, Zhang B, Yang HJ, Xie XM, Tang ZH, Li H, He JJ, Fan JH and Qiao YL. Breast cancer stage at diagnosis and area-based socioeconomic status: a multicenter 10-year retrospective clinical epidemiological study in China. BMC Cancer 2012; 12: 122.

[15] Chen CL, Hu GY, Mei Q, Qiu H, Long GX and Hu GQ. Epidermal growth factor receptor-targeted ultra-small superparamagnetic iron oxide particles for magnetic resonance molecular imaging of lung cancer cells in vitro. Chin Med J (Engl) 2012; 125: 2322-8.

[16] Hwang KP, Green JD, Li D, Simonetti OP, Resnick SA, Finn JP, Duerk JL and Omary RA. Minimizing contrast agent dose during intraarterial gadolinium-enhanced MR angiography: in vitro assessment. J Magn Reson Imaging 2002; 15: 55-61.
[17] Sahibzada I, Batura D and Hellawell G. Validating multiparametric MRI for diagnosis and monitoring of prostate cancer in patients for active surveillance. Int Urol Nephrol 2016; 48: 529-33.
[18] Zhou FF, Zhou Z and Zhai Q. MRI diagnosis of prostate cancer. Public Medical Forum Magazine 2011; 15: 70.
[19] Boehm K, Schiffmann J, Tian Z, Lesmana H, Larcher A, Mandel P, Karakiewicz PI, Graefen M, Schwarz R, Krull A and Tilki D. Five-year biochemical recurrence-free and overall survival following high-dose-rate brachytherapy with additional external beam or radical prostatectomy in patients with clinically localized prostate cancer. Urol Oncol 2016; 34: 119, e11-8.
[20] Dirani M, Nasreddine W, Abdulla F and Beydoun A. Seizure control and improvement of neurological dysfunction in lafora disease with perampanel. Epilepsy Behav Case Rep 2014; 2: 164-6.
[21] He GS, Xie SZ and Zhu XL. Research status of lovastinib in the treatment of advanced liver cancer. Journal of Logistics University of PAP (Medical Sciences) 2017; 2: 181-184.
[22] Phillips R. Prostate cancer: MRI reduces low-risk prostate cancer diagnosis and biopsy. Nat Rev Urol 2014; 11: 245.
[23] Afshar-Oromieh A, Haberkorn U, Schlemmer HP, Fenchel M, Eder M, Eisenhut M, Hadaschik BA, Kopp-Schneider A and Rothke M. Comparison of PET/CT and PET/MRI hybrid systems using a 68Ga-labelled PSMA ligand for the diagnosis of recurrent prostate cancer: initial experience. Eur J Nucl Med Mol Imaging 2014; 41: 887-97.
[24] Rosi G, Indino EL, Salvo V, Colarieti A, Fierro D, Scialpi M and Panebianco V. Role of multiparametric MRI in the diagnosis of prostate cancer: update. Urologia 2016; 83: 61-7.
[25] Azahaf M, Haberley M, Betrouni N, Ernst O, Behal H, Duhamel A, Ouzzane A and Puech P. Impact of arterial input function selection on the accuracy of dynamic contrast-enhanced MRI quantitative analysis for the diagnosis of clinically significant prostate cancer. J Magn Reson Imaging 2016; 43: 737-49.
[26] Delgado Oliva F, Arlandis Guzman S, Bonillo Garcia M, Broseta Rico E and Boronat Tormo F. Diagnostic performance of power doppler and ultrasound contrast agents in early imaging-based diagnosis of organ-confined prostate cancer: is it possible to spare cores with contrast-guided biopsy? Eur J Radiol 2016; 85: 1778-1785.
[27] Haider MA, Yao X, Loblaw A and Finelli A. Multiparametric magnetic resonance imaging in the diagnosis of prostate cancer: a systematic review. Clin Oncol (R Coll Radiol) 2016; 28: 550-67.
[28] Mendhiratta N, Taneja SS and Rosenkrantz AB. The role of MRI in prostate cancer diagnosis and management. Future Oncol 2016; 12: 2431-2443.
[29] Li P, Huang Y, Li Y, Cai L, Ji GH, Zheng Y and Chen ZQ. Application evaluation of multi-parametric MRI in the diagnosis and differential diagnosis of early prostate cancer and prostatitis. Zhonghua Yi Xue Za Zhi 2016; 96: 2973-2977.
[30] Guimaraes GC, Costa WH, Rosa RA, Zequi S and Favaretto R. Predictive role of trimprob associated with multiparametric MRI in the diagnosis of prostate cancer. Int Braz J Urol 2017; 43: 29-35.
[31] Siegel C. Re: diagnosis of extracapsular extension of prostate cancer on prostate MRI: impact of second-opinion readings by subspecialized genitourinary oncologic radiologists. J Urol 2016; 195: 96-7.
[32] Distler F, Radtke JP, Kesch C, Roethke M, Schlemmer HP, Roth W, Hohenfellner M and Hadaschik B. Value of MRI/ultrasound fusion in primary biopsy for the diagnosis of prostate cancer. Urologe A 2016; 55: 146-55.
[33] Li TF, Deng YJ and Yang BQ. Study on MRI liver targeting nano contrast agent. 2003 Symposium on preparation and technology application of nano powder in China 2003.
[34] Yu LL, Zhuang JQ and Zhang HM. Progress in application of magnetic iron oxide nanoparticle contrast agent in MRI. Chinese Journal of Laboratory Diagnosis 2011; 15: 2184-2186.
[35] Zhou ZJ. Basic research of high performance magnetic resonance contrast agent based on iron oxide nanoparticles. Xiamen University 2015.
[36] Wen G, Zhang XL, Chang RM, Xia Q, Cang P and Zhang Y. Superparamagnetic iron oxide (Feridex)-enhanced MRI in diagnosis of focal hepatic lesions. Di Yi Jun Yi Da Xue Xue Bao 2002; 22: 451-2.
[37] Wang L, Jianping LU and Wang FJ. SPIO Enhanced MRI diagnosis of hepatic focal nodular hyperplasia. Journal of Clinical Radilolgy 2002.
[38] Rao YF, Li HT and Cao GH. Research progress of superparamagnetic iron oxide nanoparticles as magnetic resonance imaging contrast agents. Chinese Pharmaceutical Journal 2014; 49: 1291-1294.